

Electronic Supplementary Information

***In situ* formation of porous graphitic carbon wrapped MnO/Ni microspheres
network as binder-free anodes for high-performance lithium-ion batteries**

Xiangzhong Kong,^a Anqiang Pan,^{*a} Yaping Wang,^a Dinesh Selvakumaran,^a Jiande Lin,^a Xinxin
Cao,^a Shuquan Liang^{* a} and Guozhong Cao^{* ab}

^a School of Materials Science & Engineering, Central South University, Changsha, Hunan, 410083,
China

^b Department of Materials Science & Engineering, University of Washington, Seattle, WA, 98195,
USA

* Corresponding author.

E-mail addresses: pananqiang@csu.edu.cn; lsq@csu.edu.cn; gzcao@u.washington.edu.

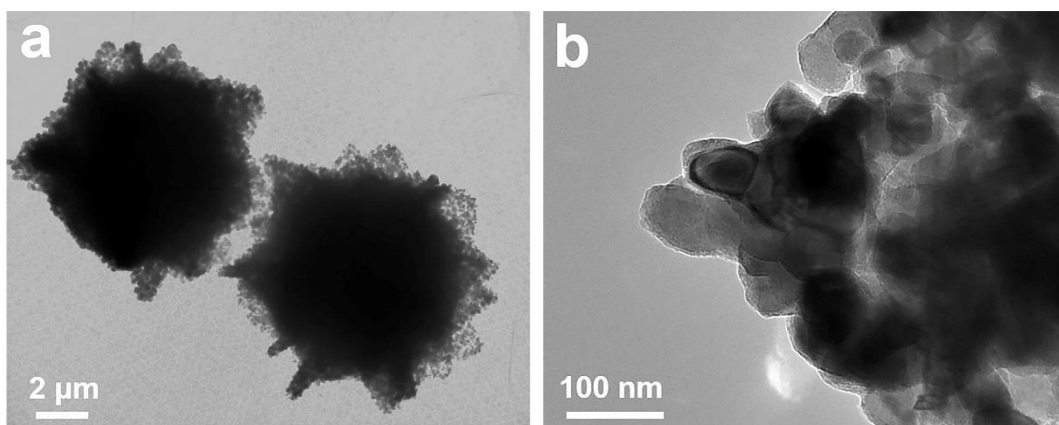


Fig. S1. SEM image (a, b) of the $\text{Mn}_{0.78}\text{Ni}_{0.22}\text{CO}_3$ after annealing in Ar at 500 °C for 2 h.

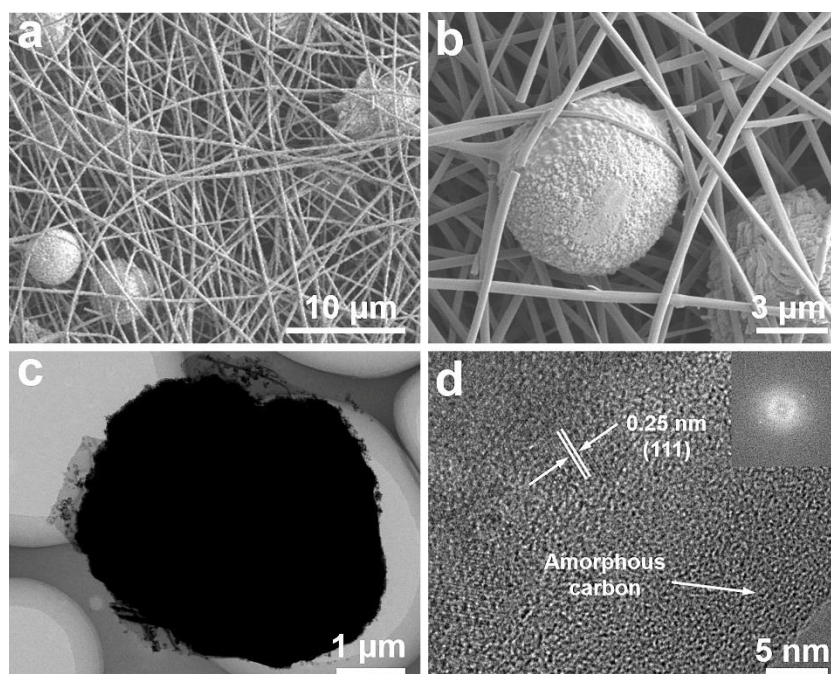


Fig. S2. SEM (a, b) and TEM (c, d) images of the MnO/ CNF.

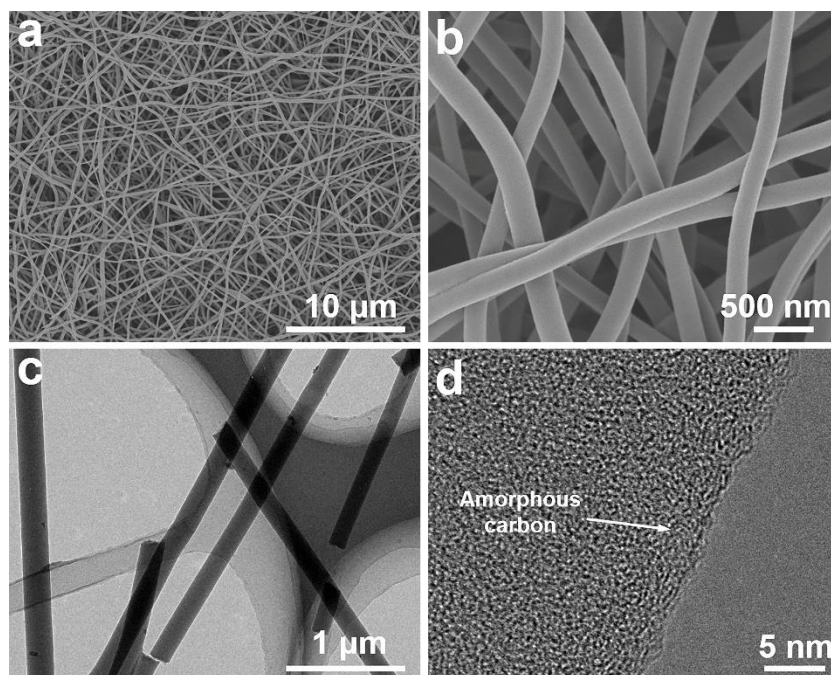


Fig. S3. SEM (a, b) and TEM (c, d) images of the CNF.

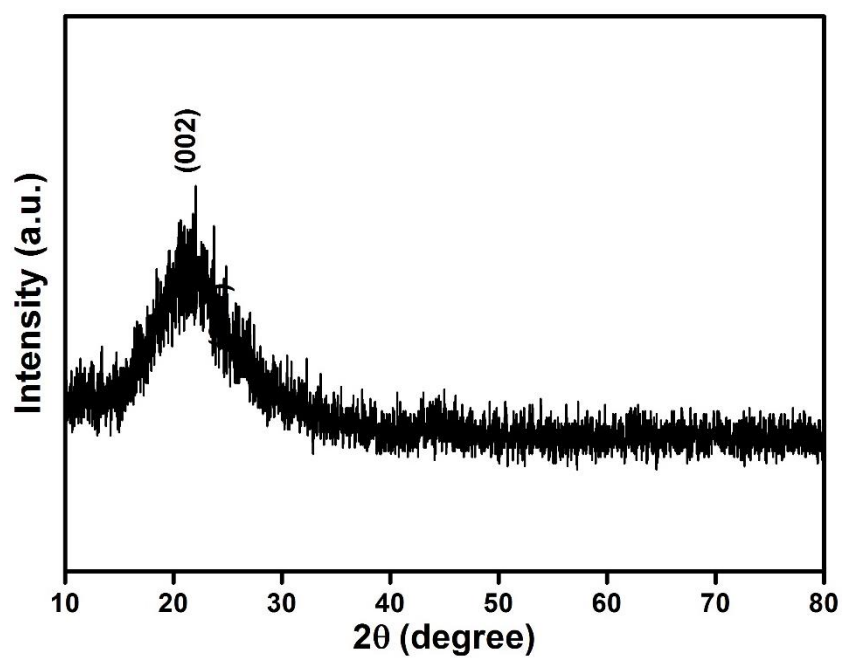


Fig. S4. The XRD pattern of the MnO/Ni/CNF after etching with 1 M HCl.

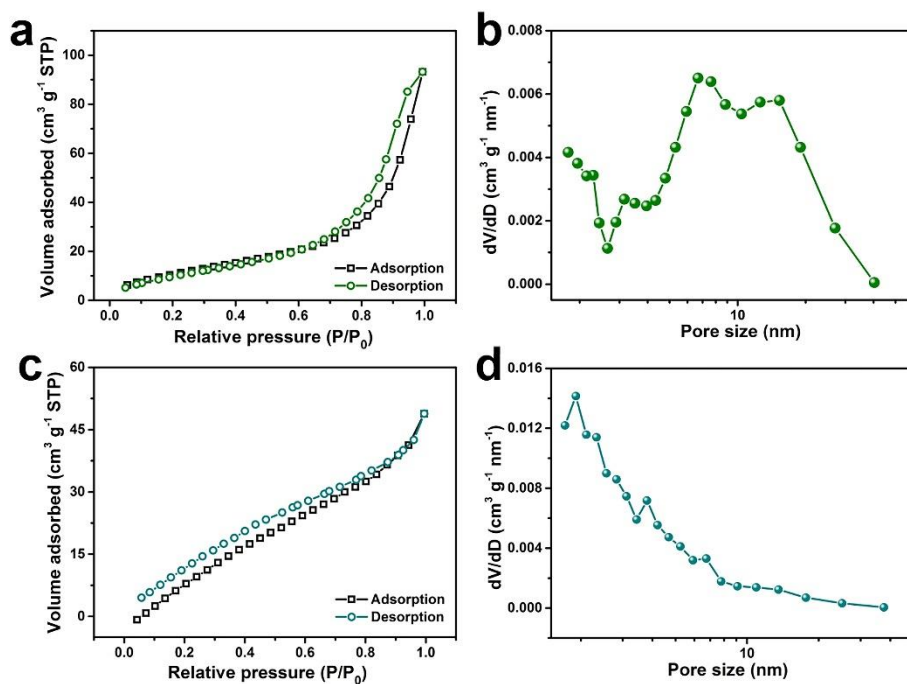


Fig. S5. Nitrogen adsorption-desorption isotherm and the corresponding pore-size distribution of the MnO/CNF (a, b) and CNF (c, d), respectively.

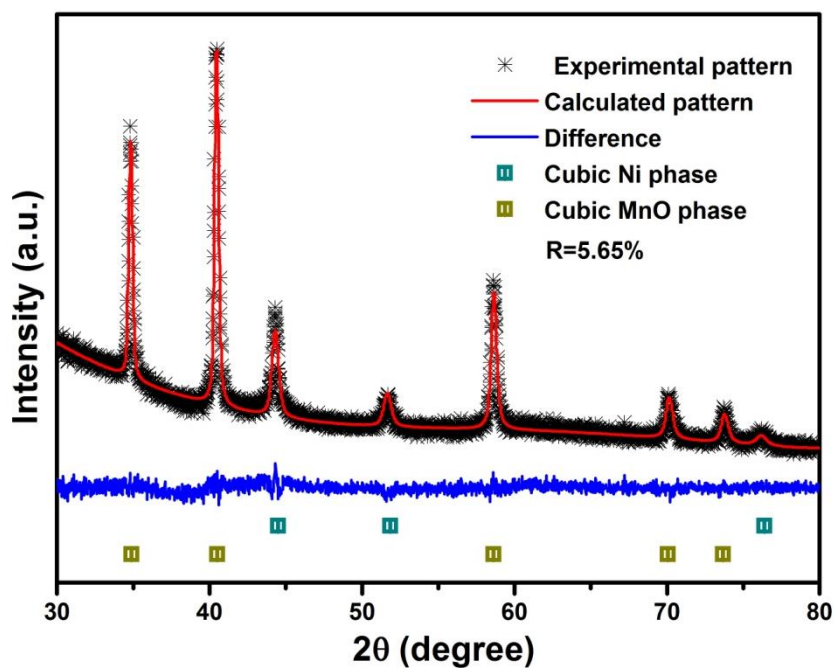


Fig. S6. X-ray diffraction pattern with Rietveld refinement of the MnO/Ni/CNF from 30 to 80°.

Table S1. Refined unit cell lattice parameters of the Ni and MnO in MnO/Ni microspheres and the standard date of Ni (426960-ICSD) and MnO (162039-ICSD).

Sample	Lattice parameters					Phase content (wt%)	R (%)
	a (Å)	b (Å)	c (Å)	β (°)	V(Å ³)		
Ni in MnO/Ni microspheres	3.52929	3.52929	3.52929	90	44.00	20.5	5.85
Ni	3.52410	3.52410	3.52410	90	43.77	—	—
MnO in MnO/Ni microspheres	4.44166	4.44166	4.44166	90	87.60	79.5	5.42
MnO	4.45100	4.45100	4.45100	90	88.18	—	—

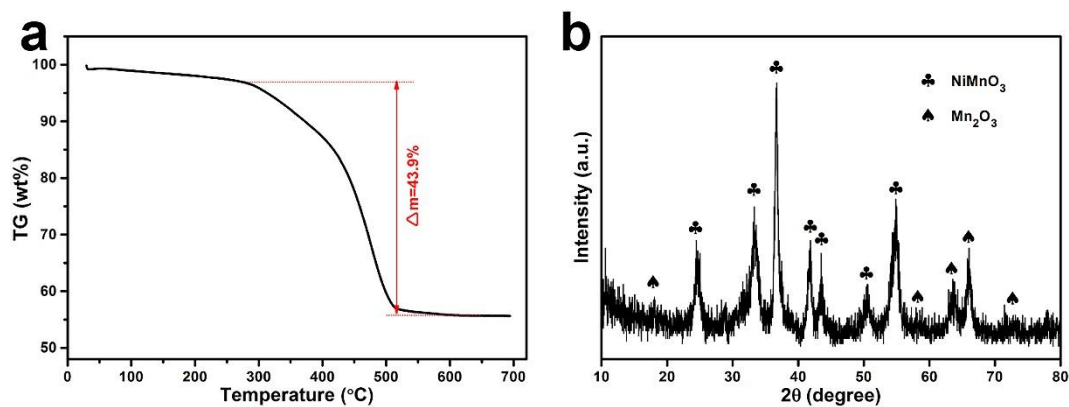


Fig. S7. (a) TG result of the MnO/Ni/CNF from room temperature to 700 °C in air. (b) XRD pattern of the MnO/Ni/CNF after annealing in air at 700 °C.

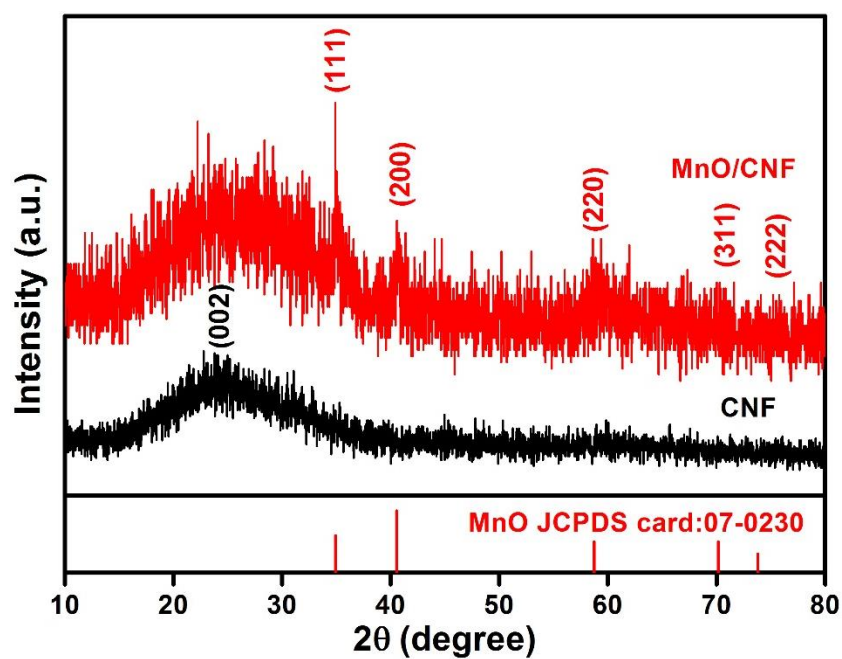


Fig. S8. XRD patterns of the MnO/CNF and CNF.

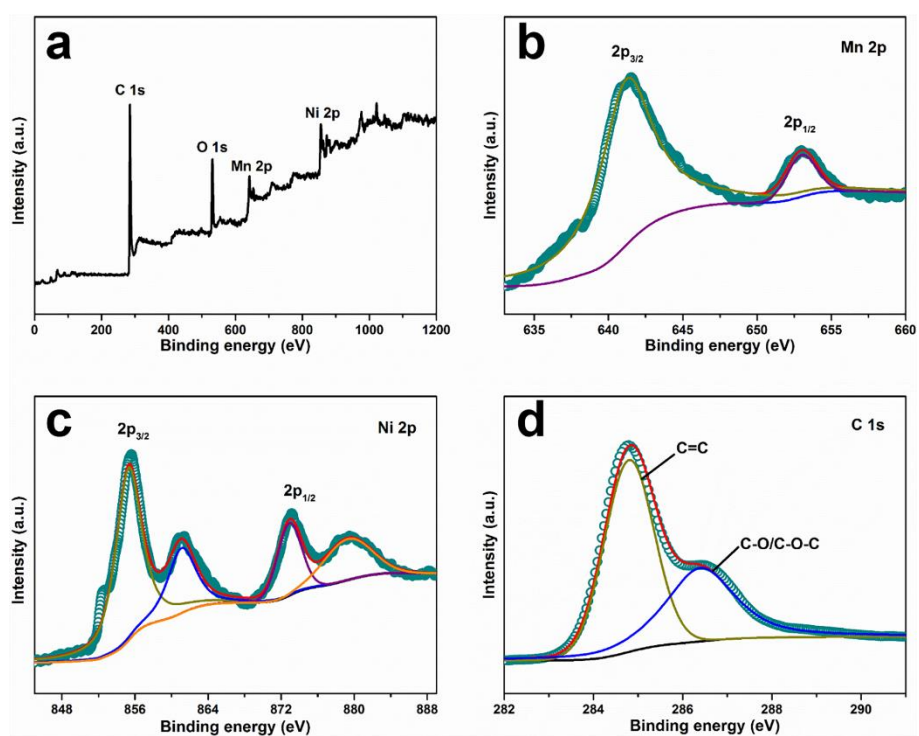


Fig. S9. (a) Survey XPS spectrum, (b) Mn 2p high-resolution spectrum, (c) Ni 2p high-resolution, (d) C 1s high-resolution spectrum of the MnO/Ni/CNF.

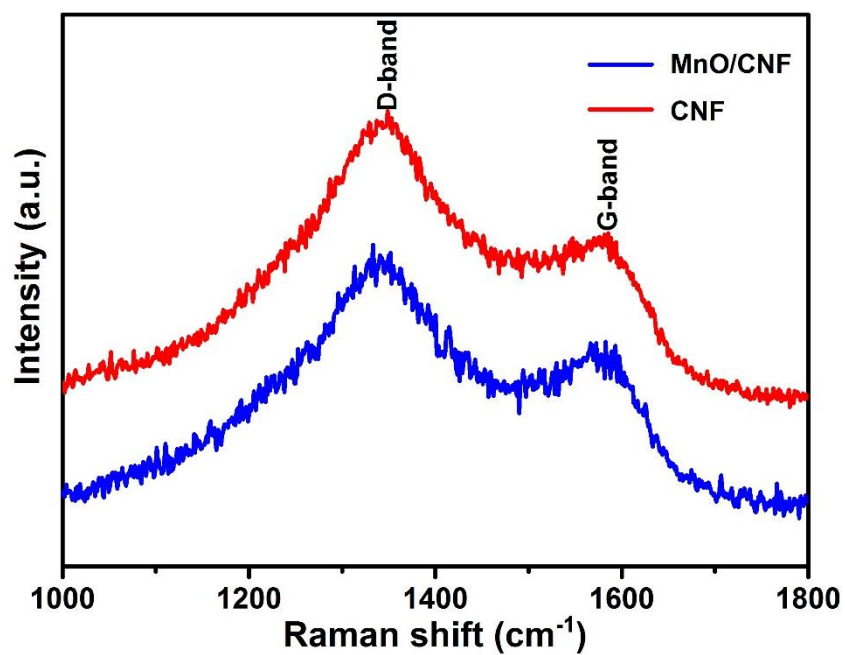


Fig. S10. The Raman spectrums of the MnO/CNF and CNF.

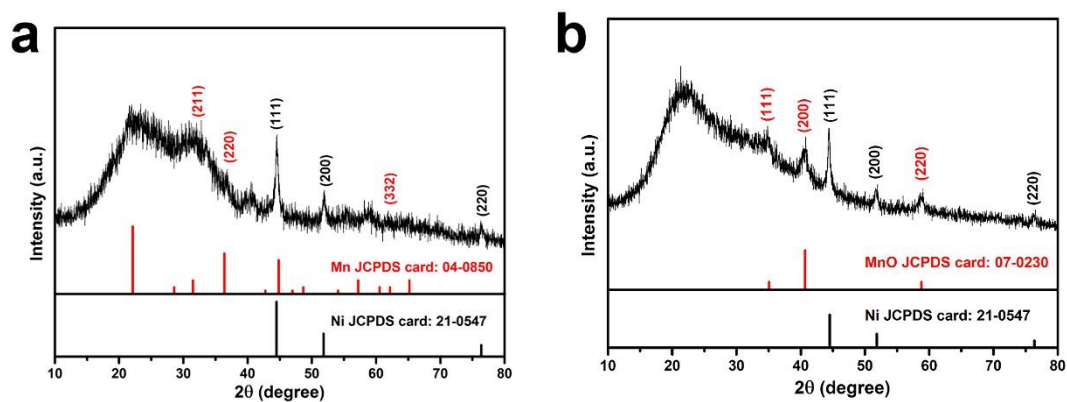


Fig. S11. XRD patterns of the MnO/Ni/CNF electrode after discharge to 0.01 V (a) and charge to 1.4 V (b).

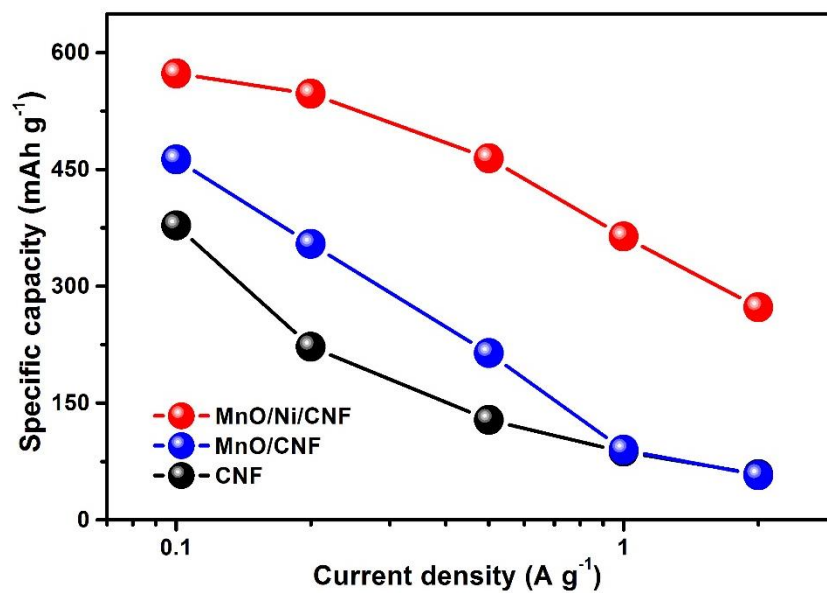


Fig. S12. Comparison of the rate performances of the MnO/Ni/CNF, MnO/CNF and CNF electrodes.

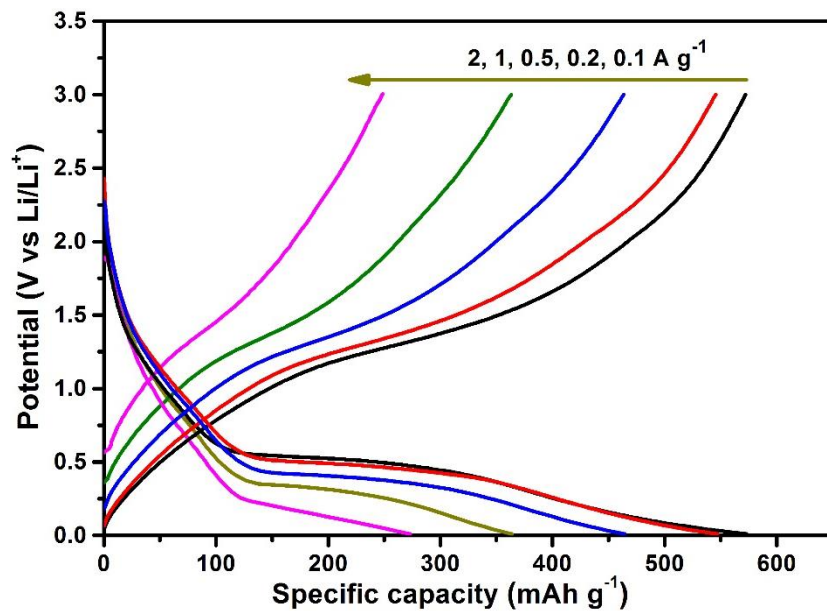


Fig. S13. Charge-discharge profiles of the MnO/Ni/CNF electrode at various rates.

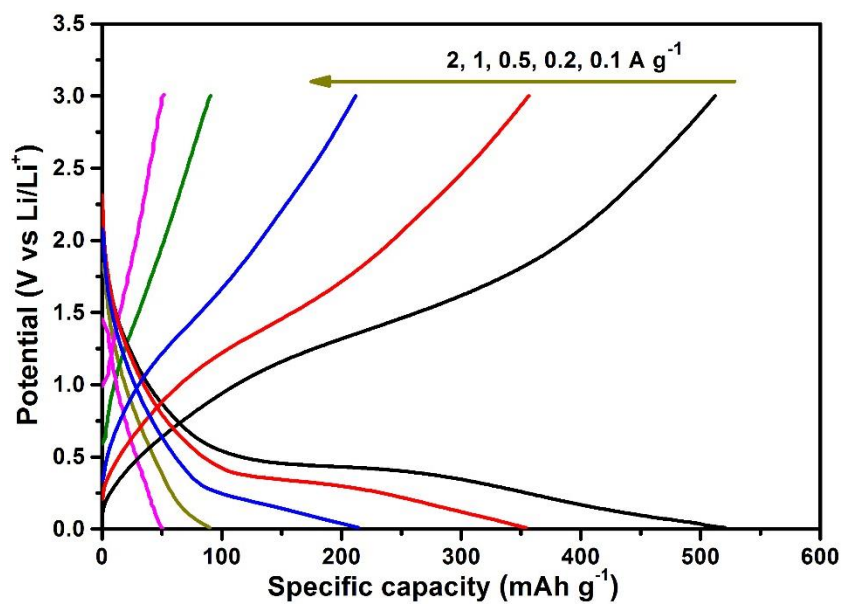


Fig. S14. Charge-discharge profiles of the MnO /CNF electrode at various rates.

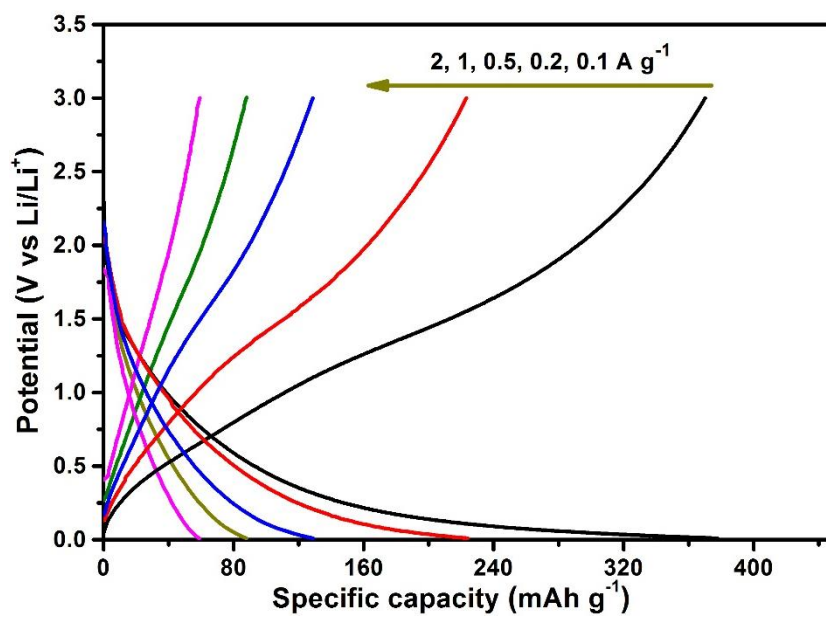


Fig. S15. Charge-discharge profiles of the CNF electrode at various rates.

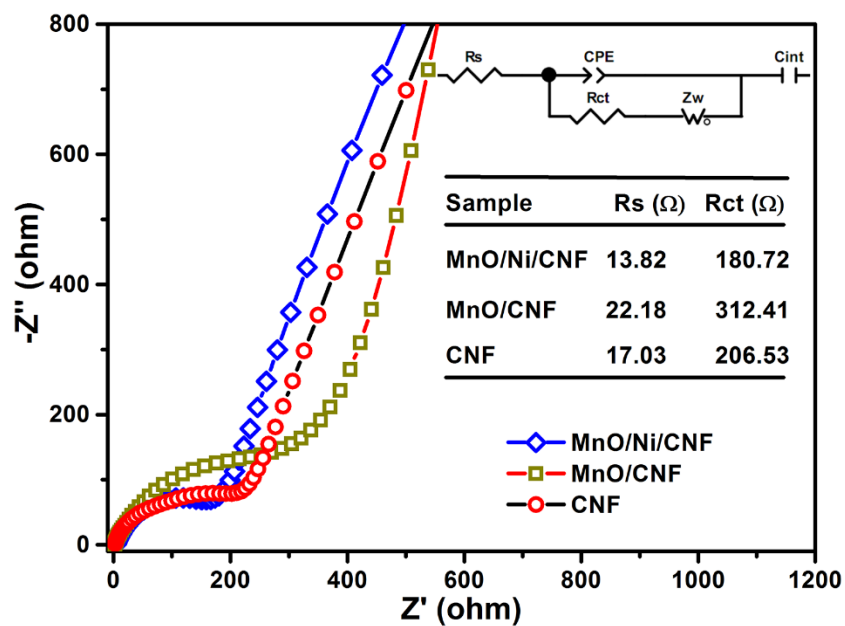


Fig. S16. Nyquist plots of MnO/Ni/CNF, MnO/CNF and CNF electrodes, respectively. The inset is the corresponding equivalent circuit model and the calculated values.

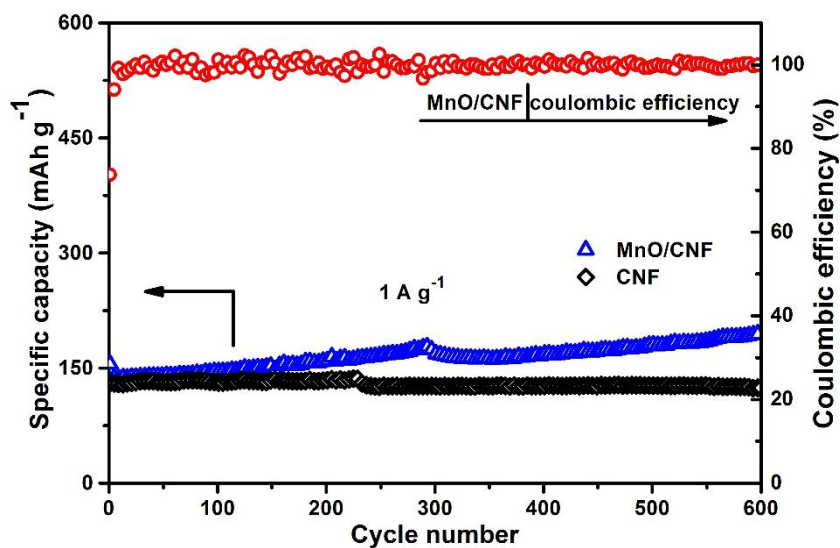


Fig. S17. Long-term cycling performances of the MnO/CNF and CNF electrodes at 1 A g^{-1} .

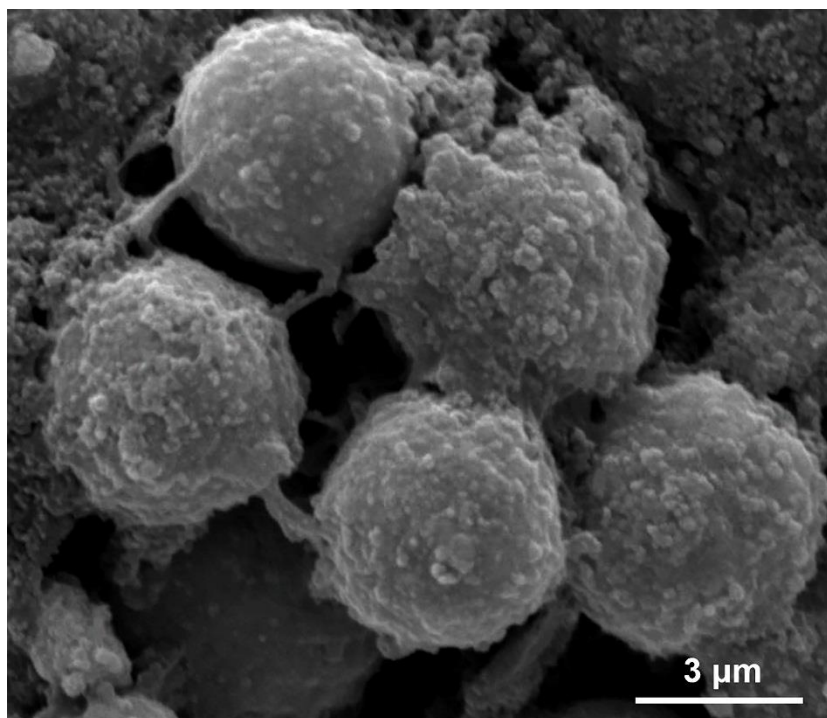


Fig. S18. SEM image of the sample without electrospinning treatment after 600 cycles at 1 A g⁻¹.

Equation S1:

The apparent diffusion coefficients of Li⁺ ions are calculated based on the Randles Sevcik equation:

$$I_p = 2.69 \times 10^5 n^{3/2} A D^{1/2} \nu^{1/2} C_0^* \quad (1)$$

Where I_p is the peak current (A), n is the number of electrons per species reaction ($n=1$, for Li⁺ ions), A is the active surface area of the electrode (1 cm² in this work), D is the diffusion coefficient of Li⁺ ions (cm² s⁻¹), ν is the scan rate (V s⁻¹), and C_0^* is the concentration of Li⁺ in the anode (mol cm⁻³).